Refereed Proceedings

The 12th International Conference on Fluidization - New Horizons in Fluidization Engineering

Engineering Conferences International *Year* 2007

Evaluation of Assisted Fluidization of Nanoagglomerates by Monitoring Moisture in the Gas Phase and the Influence of Gas Viscosity

Jose Quevedo
NJIT

Daniel Lepek
NJIT

Robert Pfeffer
NJIT, pfeffer@njit.edu

Rajesh N. Dave
NJIT

EVALUATION OF ASSISTED FLUIDIZATION OF NANOAGGLOMERATES BY MONITORING MOISTURE IN THE GAS PHASE AND THE INFLUENCE OF GAS VISCOSITY

[1]Jose Quevedo, [1]Daniel Lepek, [2]Jürgen Flesch, [1]Robert Pfeffer, [1]Rajesh N. Dave
[1]Department of Chemical Engineering, New Jersey Institute of Technology, Newark, NJ 07102
[2]Thai Aerosil Co., Ltd. Rayong 21130, Thailand

ABSTRACT

We have previously reported that the fluidization of nanoparticle agglomerates can be enhanced by the addition of external force fields such as vibration, acoustic waves, centrifugal force, and magnetic particles. The criteria usually used to evaluate the enhancement in fluidization quality are the fluidized bed expansion, pressure drop, and visual appearance of the fluidized bed to determine the presence of bubbles, large heavy agglomerates and/or channeling and spouting. Here we introduce a different approach based on measuring the rate of absorption/desorption of moisture (humidification/drying) of hydrophilic fluidized nanopowders.

The fluidizing gas was humidified in a controlled manner, and the amount of moisture in the gas phase was measured before and after the fluidized bed by humidity sensors. The experiments show that the amount of moisture adsorbed or desorbed by the bed of powder is larger when the fluidized bed was assisted by vibration or moving magnetic particles than when the bed was conventionally fluidized. In addition, the effect of high temperature gas on the fluidization of nanopowders was studied by using neon as a fluidizing gas at room temperature. It is shown that due to the increase in gas viscosity, the minimum bubbling velocity is increased, bubbling is reduced and a smoother fluidization is obtained.

INTRODUCTION

Nanoparticles and nanocomposites have become the focus of many research studies due to the unique properties of nanostructured materials that make them attractive to various industrial applications. However, before processing of nanostructured materials in the dry state can take place, the nanosized particles have to be well dispersed. Fluidization is one of the best techniques available to disperse and process powders, but fluidization of nanosized powders is expected to be difficult due to cohesive forces that become more prominent as the particle size decreases (1, 2). However, silica nanoparticles, for example, can be fluidized due to the formation of relatively large, 200-400 micron, very porous, hierarchical fractal agglomerates. These large "complex" fluidized agglomerates are composed of smaller sub-agglomerates or "simple" agglomerates, which are composed of even smaller primary agglomerates, which are made up of net-like structures of sintered chains of individual silica nanoparticles. Conventional fluidization of these nanoagglomerates has been reported by several research groups (3-5), and has been classified according to their fluidization behavior. When the fluidization is smooth, without bubbles, and a large bed expansion is observed, it is classified as Agglomerate Particulate Fluidization (APF). However, when fluidization occurs at very high minimum fluidization velocities, with bubbles and spouting, and the bed expansion is very limited, it is classified as Agglomerate Bubbling Fluidization (ABF). We have previously reported (6-9) that introducing an external force such as sound waves, rotation, vibration and/or moving magnetic particles under the influence of an oscillating magnetic field can significantly improve the fluidizability of cohesive nanopowders, reducing the minimum fluidization velocity, eliminating plug formation, channeling and spouting,

The 12th International Conference on Fluidization - New Horizons in Fluidization Engineering, Art. 48 [2007]

and resulting in a smooth, homogeneous, virtually bubbleless fluidization with negligible elutriation.

The fluidization behavior of nano-agglomerates is usually evaluated based on the bed expansion, pressure drop and the visual appearance of the bed to determine the presence of bubbles, large agglomerates or clusters and/or channeling and spouting. Here we determine the quality of fluidization by studying the amount of moisture adsorbed/desorbed by the powder, with or without the presence of an external field to assist the fluidization The amount of moisture adsorbed/desorbed by the powder depends on the amount of powder exposed to the gas phase carrying the moisture, and therefore provides information on the degree of mixing in the fluidized bed.

In addition to the humidification/drying studies, the effect of gas viscosity on fluidization is evaluated by using a fluidizing gas with a higher viscosity such as neon. It is well known that the viscosity of a gas increases with temperature and that many industrial processes involving fluidization occur at temperatures much higher than ambient resulting in an increase in viscosity in the fluidizing gas. The purpose of using neon is to reproduce fluidization at higher temperatures due to its higher viscosity (μ= 3.21x10^{-}5 Pa-s) compared to nitrogen (μ = 1.79x10^{-}5 Pa-s) at room temperature.

EXPERIMENTS

A weighed amount of dry fluidized nanopowder is humidified with a nitrogen gas stream that contains a constant amount of moisture. After the moisture in the powder has reached equilibrium with the moisture in the gas, i.e., the moisture at the top of the bed is equal to the moisture at the bottom, humidification is stopped, and dry gas is sent through the fluidized bed. The amount of moisture released by the bed of powder is monitored by measuring the moisture content of the gas stream leaving the fluidized bed as a function of time. Based on the procedure described above, an experimental system was designed and built as shown in Figure 1.

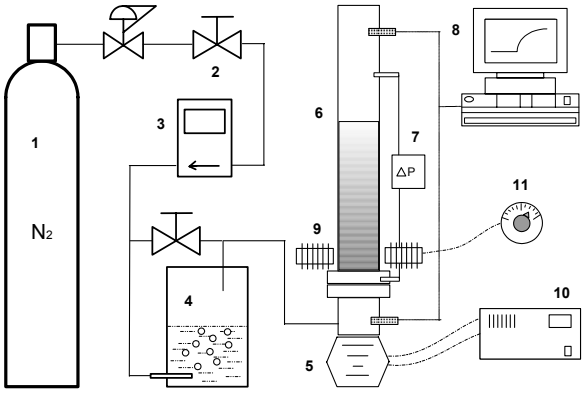

Figure 1. Schematic of the experimental apparatus for evaluating the drying process in a fluidized bed of nanopowder. (1)Gas cylinder with pressurized N_2; (2) valve; (3) mass flowmeter; (4) humidifier; (5) vibrating device; (6) fluidized bed column; (7) pressure drop display; (8) data acquisition system for humidity sensors; (9) electromagnetic coils; (10) control unit for the vibrator; (11) voltage regulator for the electromagnetic coils.

The fluidization column diameters were 3 inches for the vibrated bed and 2.5 inches for the magnetically assisted bed. The height of the columns was 5 feet. A sintered metal plate with pore size of about 100 μm and thickness of 2 mm was used as the gas distributor in each column. Taps were drilled in the columns for the humidity sensors and differential pressure transmitters. A flow of dry nitrogen gas, supplied by a pressurized gas cylinder, was adjusted by a needle valve and measured by a mass flowmeter. The flow of nitrogen gas could be directed towards the humidifier or directly to the fluidized bed depending on the stage of the experiment. This could be done by a switching valve that bypassed the humidifier. Humidification of the gas was achieved by bubbling the dry gas through water in the humidifier.

An oscillating magnetic field was generated by two electromagnetic coils that surrounded the column right above the distributor (as seen in Figure 1). The oscillating magnetic field excites 3 mm in diameter barium ferrite magnetic particles placed on the distributor causing them to translate and rotate. However, the magnetic particles do not fluidize along with the powder and tend to remain at the bottom of the bed. The intensity of the magnetic field was controlled by

adjusting the voltage of the power supply to the electromagnetic coils and its value oscillated between 150 and 300 Gauss. For vertically vibrated assisted fluidization a Ling Dynamic system was used; the intensity of the vibration was adjusted to about 3 to 5 times normal gravity (g), and the frequency of the oscillation was of the order of 60 to 100 Hz. More details on the setup corresponding to the magnetic assistance and the vibration can be found in (6, 9).

Two different kinds of nanopowders supplied by Degussa were used in the experiments: Aerosil® 200, that can be readily fluidized as agglomerates and shows APF behavior and Aerosil® 90, which is difficult to fluidize homogeneously (ABF behavior) and contains a large fraction of large agglomerates (over 1 mm diameter). Both powders are hydrophilic, and in some experiments, the powders were sieved before placing them into the fluidization column using sieve orifice sizes of 500 μm and 700 μm.

For the high viscosity gas experiments, the fluidization column was 2 inches in diameter and 5 feet high. The distributor is a sintered stainless steel plate 2 mm thick having a pore size of 20 μm. A cloth filter is located at the top of the column to prevent any elutriated powder from leaving the column. It is important to note that in these experiments no moisture was added to the fluidizing gas. Two types of nanopowders supplied by Degussa, which show contrasting fluidizing behavior, were tested. Aerosil® R974 is a hydrophobic silica exhibiting agglomerate particulate fluidization (APF) behavior, has a bulk density of 33 kg/m^3, a material density of 2250 kg/m^3, and a primary particle size of 12 nm. Aeroxide® TiO_2 P25 is hydrophilic, has a bulk density of 128 kg/m^3, a material density of 4500 kg/m^3, a primary particle size of 21 nm and exhibits agglomerate bubbling fluidization (ABF) behavior Prior to charging the powder into the column, the nanopowders were sieved by using a 40-mesh sieve opening (about 425 μm). Data regarding the flow of the fluidizing gas, fluidization quality, bubbling, bed pressure drop and bed height were collected for both nanopowders, but only the results for Aerosil® R974 are presented below.

RESULTS AND DISCUSSION

The humidity sensors at the bottom and the top of the fluidization column provided data on the temperature, relative humidity and dew point of the gas at least every 2 seconds, a time interval that could be adjusted. The dew point data are used to obtain the absolute humidity in the gas entering and leaving the fluidized bed as a function of time by calculating the partial pressure of water in the gas. The time-dependent moisture data from the sensor at the top of the bed was used for finding the total amount of moisture adsorbed by the bed of powder. Figure 2 shows the absolute humidity data collected from the sensor at the bottom in red and the sensor at the top in blue during a long term experimental run. Clearly, two regions can be identified. The humidification of the powder occurs when a certain amount of moisture is detected by the sensor at the bottom (red line) and the drying occurs when the sensor at the bottom (red line) shows zero moisture. Also, it can be seen that the powder gets saturated with moisture after about 3000 seconds. This occurs when the moisture from the sensor at the top equals the moisture of the sensor at the bottom.

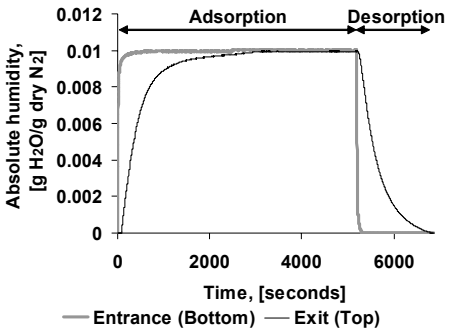

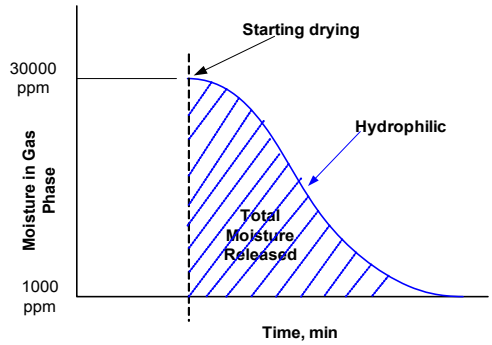

Figure 2 (left). Plot showing the absolute humidity levels in the gas phase from the sensor at the bottom (red line) and the sensor at the top (blue line) with respect to time.

Figure 3 (right). Estimation of the amount water adsorbed by the powder using data collected from the sensor at the top of the fluidized bed.

The 12th International Conference on Fluidization - New Horizons in Fluidization Engineering, Art. 48 [2007]

The drying region is of particular interest since it gives information on the amount of moisture adsorbed by the powder. Since the absolute humidity is given as a function of time, by integrating with respect to time, the total amount of moisture adsorbed by the powder can be found (as shown in Figure 3). Moreover, this quantity can be used to compare the amount of moisture adsorbed by the powder when fluidized conventionally or with assisting methods.

When the fluidized powder is humidified during a period of time long enough so that it gets saturated at a certain temperature, i.e., moisture from the sensor at the top is equal to moisture from the sensor at the bottom, the amount of moisture adsorbed by the powder is in equilibrium with the moisture in the gas phase. This amount of moisture adsorbed at equilibrium follows the adsorption isotherm of the powder at the temperature of the experiment. Therefore, the adsorption isotherm of the powder can be found by measuring the total amount of moisture adsorbed by the powder after being humidified (at a constant temperature) at different concentrations of moisture in nitrogen, or at different partial pressures of water. Adsorption isotherms at room temperature were found for both powders, Aerosil® 200 and Aerosil® 90, as shown in Figure 4. While most of the experiments were run at a gas velocity of 1.54 cm/s, one experimental run in each case was done at a higher gas velocity (1.74 cm/s) to verify that the isotherm is not dependent on the gas velocity. In order to validate the adsorption isotherm data obtained by monitoring the moisture in the gas phase, the adsorption isotherms were also obtained using a gravimetric method. Data collected using the gravimetric method is shown in Figure 5 for Aerosil® 200 and Aerosil® 90. Although not exactly the same (because the gravimetric method only uses a sample of powder that is fully fluidized), the isotherms obtained by both methods are quite similar.

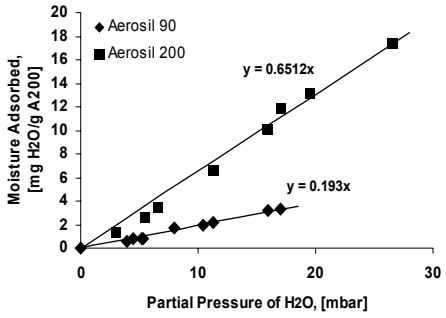

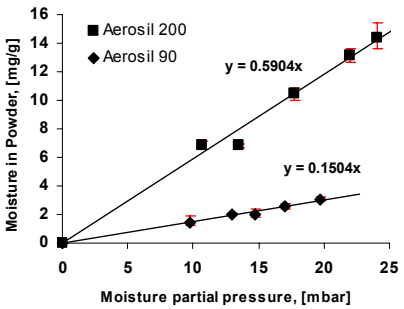

Figure 4 (left). Experimental data collected and linear regression for the adsorption isotherm of Aerosil® 200 and Aerosil® 90 found by monitoring moisture in the gas phase.
Figure 5 (right). Adsorption isotherms at room temperature found by the gravimetric method for Aerosil® 200 and Aerosil® 90.

Short Time Humidification Experiments

The effects of assistance in the fluidized bed can be readily seen (even in short time experiments) because the dynamics of the powder, i.e., movement and mixing of the powder with the gas phase in a conventional fluidized bed is poorer than in an assisted fluidized bed. An example of the results obtained in the short-time experiments is given for Aerosil® 200 when the partial pressure was about 57 mbar measured by the sensor at the top, with a gas velocity of 1.5 cm/s and a temperature of about 128° F. It is important to note that the gas velocity corresponds to the minimum fluidization velocity (U_{mf}) of a vibrated fluidized bed of powder which is lower than the U_{mf} of a conventionally fluidized bed. The effect of vibration on the fluidized bed is shown qualitatively in Figure 6. This figure shows that during humidification (high moisture at the bottom), the sensor at the top of the bed picks up a delay, which is shorter when fluidizing without assistance, indicating gas bypassing in the bed. The delay is longer for vibration assisted fluidization, indicating that there is less gas bypassing in the fluidized bed and hence better mixing. Another characteristic shown in Figure 6 is that by assuming that the drying process starts at the inflection point of the drying data (light and dark blue lines), the total moisture adsorbed by the powder can be estimated by finding the area under the curve. Figure 7 shows

the cumulative moisture released by the powder with respect to time based on drying data from Figure 6. As seen in Figure 7, the fluidized bed of powder retains more moisture and releases it quicker when vibration is applied, a clear indication of the enhancement of the dynamics of the fluidized bed by the assisting method.

Long Time Humidification Experiments

One of the major objectives of these experiments was to compare the drying rates of powder while fluidized in a conventional or an assisted fluidized bed; therefore, the powder has to be equally humidified in all the runs. To satisfy this requirement, the powder was humidified until saturation, and thus longer humidification times were required. Figure 8 shows a comparison of the cumulative moisture data obtained during drying of Aerosil® 200; it can be seen that when the powder was vibrated during fluidization it adsorbs more moisture and releases it faster than when using conventional fluidization. However, when magnetic assistance is applied, the powder also dries faster than under conventional fluidization, but does not release as much moisture, Since the magnetic assistance acts only at the bottom of the fluidized bed, any powder that attaches to the wall of the column will not participate in the fluidization process, thus reducing the total amount of moisture adsorbed and released during drying.

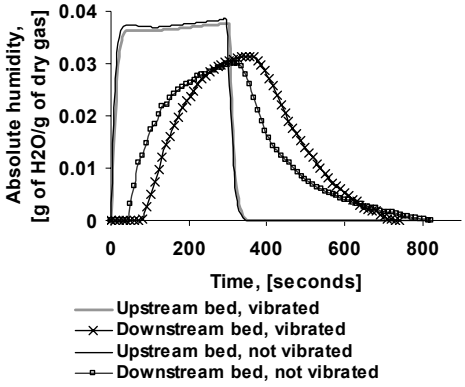

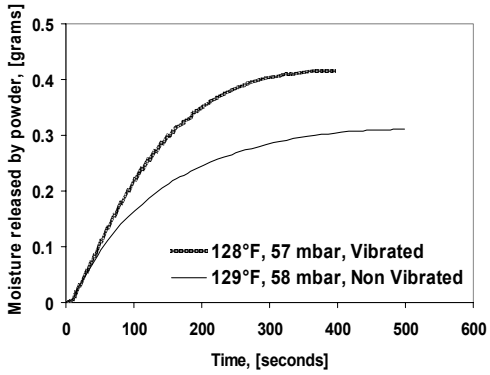

Figure 6 (left). Data from two short time experiments for assessing the impact of vibration. 40 grams of Aerosil® 200 were humidified for about 5 minutes.
Figure 7 (right). Comparison of the amount of moisture released by the powder with respect to time for a conventional and a vibrated fluidized bed.

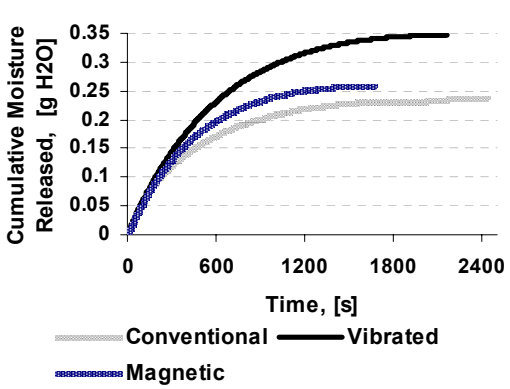

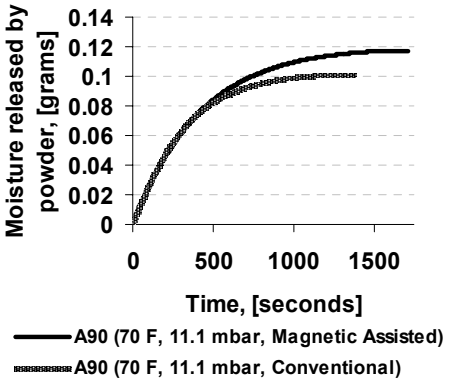

Figure 8 (left). Effect of vibration and magnetic assistance on fluidization during drying process of Aerosil® 200 (not sieved).
Figure 9 (right). Cumulative moisture released from powder as function of time, comparing magnetic assisted and conventional fluidization during drying of Aerosil® 90 (not sieved).
Mass of powder 40 grams, gas velocity, 1.5 cm/s, humidification time, 90 minutes,

This particular problem is overcome when using vibration which acts along the entire length of the

The 12th International Conference on Fluidization - New Horizons in Fluidization Engineering, Art. 48 [2007]

column. In addition, a smooth fluidization is obtained when Aerosil® A200 is fluidized with vibration assistance regardless of whether the powder has been sieved or not. On the contrary, during conventional fluidization, channeling and bubbling occur, increasing elutriation of particles and forming some motionless regions of powder that reduce the effective mass of the fluidized powder in the bed and therefore the amount of moisture adsorbed.

Aerosil® 90 contains a much larger fraction of large agglomerates (>700 μm) than Aerosil® 200. It is believed that these large agglomerates do not allow for a good distribution of the gas in the bed causing channels and bubbles. When vibration is applied during fluidization of Aerosil® 90 without sieving (powder taken directly from the container), there is very little difference in the rate of drying as compared to conventional fluidization without vibration. One possible explanation for this observation is that the vibration intensity applied is not strong enough to break down the large agglomerates present in Aerosil® 90. When visually inspected, the fluidized bed is made of two sections, a packed bed of large agglomerates at the bottom and a spouting fluidized bed of smaller agglomerates over the packed bed. The large fraction of large agglomerates reduces the effective amount of powder that participates in fluidization and the bed of powder adsorbs less moisture than expected, apparently due to the poor mixing.

Non-sieved Aerosil® 90 was also fluidized using magnetic assistance and the rate of drying of the powder was compared to conventional fluidization as shown in Figure 9. When magnetic assistance is used, the fluidized bed of powder adsorbs more moisture (about 20 %) than during conventional fluidization. It is believed that the magnetic assistance breaks down the large agglomerates and improves the dynamics of the fluidized bed. In addition, visual inspection of the powder after being fluidized with magnetic assistance shows a significant reduction of the fraction of large agglomerates, which can even disappear entirely depending on the length of time the magnetic assistance is applied.

By making a number of reasonable assumptions, the concentration of moisture with respect to time in the gas at the exit of the fluidized bed can also be modeled and compared to the experimental data. It was assumed that a) the fluidization is homogeneous and bubbling does not occur; b) there is no concentration gradient within the agglomerate; c) the outer boundary of the agglomerate is in equilibrium with the surrounding gas phase and can be described by the adsorption isotherm; d) mixing in the fluidized bed is CSTR-like so that the concentration of moisture in the gas phase of the fluidized suspension is equal to the concentration of moisture exiting the fluidized bed, i.e., the concentration of moisture in the gas phase is independent of position in the fluidized bed. Based on these assumptions, a mass balance was applied to both phases, the agglomerates (solid phase) and the gas phase, and the two differential equations solved using Matlab. Figure 10 shows a comparison of the experimental data and the modeling results obtained in a vibrated assisted fluidized bed of Aerosil 200; more details of the modeling and the equations which were solved can be found in reference (10).

Influence of Viscosity on Fluidization

Similar fluidization characteristics were observed when both nitrogen and neon were used as the fluidizing gas when fluidizing hydrophobic Degussa Aerosil® R974 unassisted. Prior to achieving a fluidized state, both gases caused the powder to lift as a plug, which then led to the breakup of the plug into a dispersed powder. Before the powder begins to fluidize, channeling occurred for both nitrogen and neon fluidization. However as seen in Figure 11, Aerosil® R974 begins to fluidize at a slightly lower velocity with neon (U_{mf} = 0.34 cm/s) than with nitrogen (U_{mf} = 0.41 cm/s), assuming fluidization occurs at the discontinuous jump in the pressure drop. It is also observed that over time, the pressure drop of the bed begins to decrease more with neon than with nitrogen. It is believed that this occurs because the more viscous neon tends to lift fine agglomerates from the bed's surface. As seen in Figure 11, the non-dimensional pressure drop (normalized with the weight of the bed per unit area) is close to unity for fluidization with nitrogen and stays relatively constant as the velocity is increased, but decreases below unity for fluidization with neon, indicating a loss of bed particles.

From Figure 11, it can be seen that a maximum bed height ratio of 4.7 could be obtained prior to any observable elutriation when using nitrogen. For neon, the bed surface could reach 5.6 times its original bed height at similar gas velocities, indicating an even better

fluidization quality.

Using the method proposed by Valverde et al. (11) and applied to nanoagglomerates by Nam et al. [6] and Valverde and Castellanos (12), the size of the agglomerates, number of particles per agglomerate, and fractal dimension can be calculated. For a Richardson-Zaki (R-Z) index of 5.6 (13), the size of the fluidized complex agglomerates was calculated to be 309 μm and 373 μm, when fluidized with nitrogen and neon, respectively. We have previously made in situ measurements of nanoagglomerate sizes in a fluidized bed of a variety of different nanoparticles, using an optical system to image the agglomerates on the surface of the fluidized bed [4, 9]. For sieved Aerosil® R974 (particles below 500 μm) fluidized with nitrogen without assistance, the mean agglomerate size was found to be around 180 μm. This smaller value for the average agglomerate size may be due to the stratification of the fluidized bed and/or the fact that the agglomerate images are taken from the surface of the bed, which may not be representative of the agglomerate size distribution throughout the entire fluidized bed.

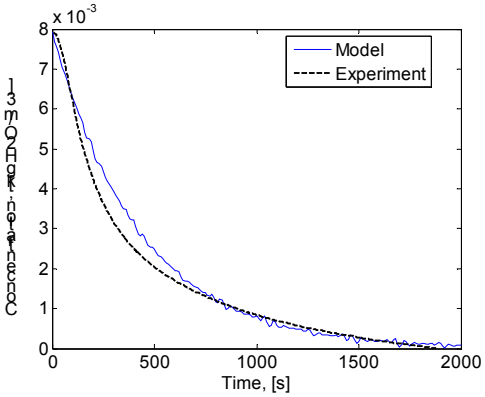

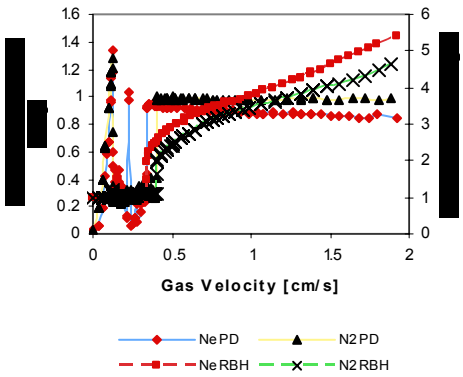

Figure 10. (left) Comparison of the experimental data and modeling results of the drying of a vibrated assisted fluidized bed of Aerosil 200.
Figure 11. (right) Pressure Drop and Reduced Bed Height vs. Superficial Gas Velocity for Aerosil® R974

When Aerosil® R974 was fluidized with nitrogen at high velocities, we observed that some bubbling occurred prior to elutriation. No bubbling was observed when neon was used; rather, the bed transits from a state of homogeneous fluidization to a turbulent regime in which fine particles are lifted from the surface of the bed and elutriated. This result is in good agreement with theory developed by Valverde et al (14) based on predicting the maximum bubble size for fluidized complex nanoagglomerates

CONCLUSIONS

Based on the fluidization behavior observed, and the results of monitoring the moisture in the gas phase during drying, fluidization of both APF and ABF fumed silica nanoparticles is clearly enhanced by applying external force field assistance. The quantification of moisture in the powders was done by monitoring the moisture in the gas phase to obtain adsorption isotherm data. Data were obtained for Aerosil® 200 and Aerosil® 90 showing that the former adsorbs more moisture than the later; results corroborated from the adsorption isotherms obtained by using the gravimetric method.

For Aerosil® 200, the presence of large agglomerates does not affect the amount of moisture retained by the fluidized bed since they are found in small amounts. However, for Aerosil® 90, large agglomerates constitute a significant fraction of the powder and they affect the adsorption of moisture due to the poor mixing between the solid and gas phases, hindering the overall absorption of moisture by the bed of powder. The enhancement of fluidization due to the assisting methods is reflected by the increase of moisture retained by the overall fluidized bed of powder during humidification and by the reduction in the time needed for the bed of powder to release the moisture trapped as shown by the drying curves obtained by monitoring the moisture

in the gas phase.

High temperature conditions required for many industrial processes result in an increase in the viscosity of the fluidizing gases. The effect of a higher gas viscosity on the fluidization of agglomerates of nanoparticles has been studied at room temperature by comparing fluidization with nitrogen and higher viscosity neon. An increase in the viscosity of the fluidizing gas leads to a better, more homogeneous fluidization as shown by the larger bed expansion observed for an APF type powder such as Aerosil® R974, and a more stable behavior at high gas velocities. The appearance of large, unstable, macro-scale bubbles has been curtailed when neon is used for fluidizing APF (silica). The experimental observations, when fluidizing nanoagglomerates with neon as compared to nitrogen, also agree qualitatively with theory to predict whether a bubble will grow or not, and with experiments performed using the different viscosity gases to fluidize fine Geldart group C micron sized particles (14, 15).

ACKNOWLEDGEMENTS

The authors gratefully acknowledge financial support from the National Science Foundation (NIRT Grant DMI-0210400). Special thanks are also due to Prof. Jose Manuel Valverde, our collaborator at the University of Seville in Spain and to Dr. Jürgen Flesch and Dr. Herbert Riemenschneider of the Degussa Corporation, which co-sponsored a part of this research.

REFERENCES

(1) S. Morooka, K. Kusakabe, A. Kobata, Y. Kato, “Fluidization State of Ultrafine Powders,” Journal of Chemical Engineering of Japan, vol. 21, pp. 41, 1988.
(2) Z. Wang, M. Kwauk, H. Li, “Fluidization of Fine Particles,” Chemical Engineering Science, vol. 53, pp. 377, 1998.
(3) Y. Wang, G. Gu, F. Wei, and J. Wu, “Fluidization and Agglomerate Structure of SiO_2 Nanoparticles,” Powder Technology, vol. 124, pp. 152, 2002.
(4) C. Zhu, Q. Yu, R. Pfeffer, R.N. Dave, “Gas Fluidization Characteristics of Nanoparticle Agglomerates,” AIChE J., vol. 51-2, pp. 426-439, 2005.
(5) L. Hakim, J. Portman, M. Casper, A. Weimer, “Aggregation Behavior of Nanoparticles in Fluidized Beds,” Powder Technology, vol 160, pp. 149-160, 2005.
(6) C. Nam, R. Pfeffer, R. N. Dave, S. Sundaresan, “Aerated Vibrofluidization of Silica Nanoparticles,” AIChE Journal, vol. 51-2, pp. 426-439, 2004.
(7) C. Zhu, G. Liu, Q. Yu, R. Pfeffer, R. Dave, C. Nam, “Sound Assisted Fluidization of Nanoparticle Agglomerates,” Powder Technology, vol. 141, pp. 119-123, 2004.
(8) J.A. Quevedo, R.N. Dave, R. Pfeffer, “Fluidization of Nanoagglomerates in a Rotating Fluidized Bed” AIChE Journal, in press, 2006.
(9) Q. Yu, J.A. Quevedo, R.N. Dave, R. Pfeffer, C. Zhu, “Enhanced Fluidization of Nanoparticles in an Oscillating Magnetic Field,” AIChE J., vol. 51, pp. 1971-1979, 2004.
(10) J.A. Quevedo, J. Flesch, R. Pfeffer, R. Dave, “Evaluation of Assisting Methods on Fluidization of Hydrophilic Nanoagglomerates by Monitoring Moisture in the Gas Phase,” submitted to Chemical Engineering Science, 2006.
(11) J. M. Valverde, M.A.S. Quintanilla, A. Castellanos, P. Mills, “The Settling of Fine cohesive Powders,” Europhysics Lett., vol 54, pp 329-334, 2001.
(12) J.M. Valverde, A. Castellanos, “Fluidization of Nanoparticles: A Modified Richardson-Zaki Law,” AIChE J., vol. 52-2, pp. 838-842, 2006.
(13) G. K. Batchelor, “Sedimentation in a Dilute Polydisperse System of Interacting Spheres. Part 1: General Theory,” J. Fluid Mech., vol. 119, pp. 379-408, 1982.
(14) J.M. Valverde, A. Castellanos, “High Viscosity Gas Fluidization of Fine Particles: An Extended Window of Quasi-Homogeneous Flow,” Phys. Rev. Lett., in press. 2006.
(15) J.M. Valverde, A. Castellanos, Daniel Lepek, Jose Quevedo, Robert Pfeffer, Rajesh N. Dave, ”The Effect of Gas Viscosity on the Fluidization of Fine and Ultrafine Particles -Theory and Experiments”, in preparation, 2006.